Light emission from the shadows: Surface plasmon nano-optics at near and far fields

S. C. Hohng, Y. C. Yoon, and D. S. Kim[a)]
School of Physics, Seoul National University, Seoul 151-742, Korea

V. Malyarchuk, R. Müller, and Ch. Lienau[b)]
Max-Born-Institute fur Nichtlineare Optik und Kurzzeitspektroskopie, Max-Born-Strasse. 2a, D-12489 Berlin, Germany

J. W. Park, K. H. Yoo, and J. Kim
Korea Research Institute of Standards and Science, Yunsung, P.O. Box 102, Taejon 305-600, Korea

H. Y. Ryu
Department of Physics, Korea Advanced Institute of Science and Technology, 373-1 Kusong-dong, Yusong-gu, Taejon 305-701, Korea

Q. H. Park
Department of Physics, Korea University, Seoul 136-701, Korea

(Received 1 May 2002; accepted 27 August 2002)

When light illuminates a thick metal film perforated with small holes, shadows appear. At the nanoscopic level, however, light can be emitted predominantly from the metal surfaces between the holes—shadows can be indeed brighter than the lighted holes. The symmetry of the near-field emission pattern is determined by the symmetry of the surface plasmon waves. Surprisingly, these nanoscopic emission patterns from the metal can be preserved to the far-field region, where the pattern becomes sinusoidal. This unusual behavior of light emission from the shadows is explained by efficient wave vector selection. © *2002 American Institute of Physics.*
[DOI: 10.1063/1.1515134]

Generally, the transmission efficiency of light through subwavelength holes is believed to be exceedingly low.[1,2] When these holes form periodic arrays, however, the transmission efficiency may be enhanced by several orders of magnitude at certain wavelengths.[3] This phenomenon has attracted much attention and recent experimental and theoretical work has attributed it to the excitation of surface-bound waves, surface plasmons (SPs),[4–6] in terms of which the spectral positions and strengths of the transmission resonances are determined.[3,7–22] With regard to the microscopic emission patterns, a recent study suggests that, for off-resonant excitation, the field intensity is localized around the holes.[10] In addition, many theoretical calculations contend that SPs interfere constructively near holes.[16,19,20]

In this letter, we present microscopic emission patterns of light transmitted through thick metal films with periodic hole arrays. We show that the dominant contribution to emission can be from the metal surfaces outside the holes. The near-field pattern also reflects the symmetry of the SP waves that are polarization controlled. Moreover, measurements reveal that the emission from the metal surfaces can reach the far-field region, where the pattern becomes sinusoidal. These experimental results clearly indicate that the near-field patterns are determined by the coherent interference of many SP waves, while efficient wave vector selection makes the far-field pattern dominated by only the first two diffraction orders.

Figure 1(a) shows a scanning electron microscopy image of a typical sample. A far-field transmission spectrum of a sample with a 150 nm hole diameter and a period of 850 nm in a 300 nm thick gold film is displayed in Fig. 1(b), with light incident on the sapphire side. It shows transmission peaks at SP resonances corresponding to surface charge oscillations at the air–metal and sapphire–metal interfaces, respectively. The 930 nm peak corresponds to the air–metal SP resonance of the first order with its symmetry along the x or y axes defined as horizontal and vertical, respectively. These are termed the [1, 0] or [0, 1] modes. The 1100 nm peak is the [1, 1] sapphire–metal SP resonance of second order with its symmetry along the axis diagonal. We employ a near-field scanning optical microscope in the transmission geometry where a Ti:sapphire laser excites the sample on the sapphire–metal side near the normal incidence and a metal-coated fiber tip with a sub-100 nm aperture collects light on the air–metal side. The incident beam is focused to a spot 5–10 μm in size on the sample. Figure 1(c) is a schematic sketch of light emission from the holes, as our macroscopic experience implies.

Figure 2 shows a near-field emission pattern for each polarization with the wavelength of an incident beam around the air–metal [1, 0] SP resonance peak as shown in Fig. 1(b). While the transmission efficiency in the far-field region is independent of polarization,[10] the near-field images show a strong polarization dependence. We observe stripes that run essentially perpendicular to the polarization direction. In addition, there are minima between the stripes, so that a peak-to-valley ratio of 10 or larger is seen. The polarization de-

a)Electronic mail: denny@phya.snu.ac.kr
b)Electronic mail: lienau@mbi-berlin.de

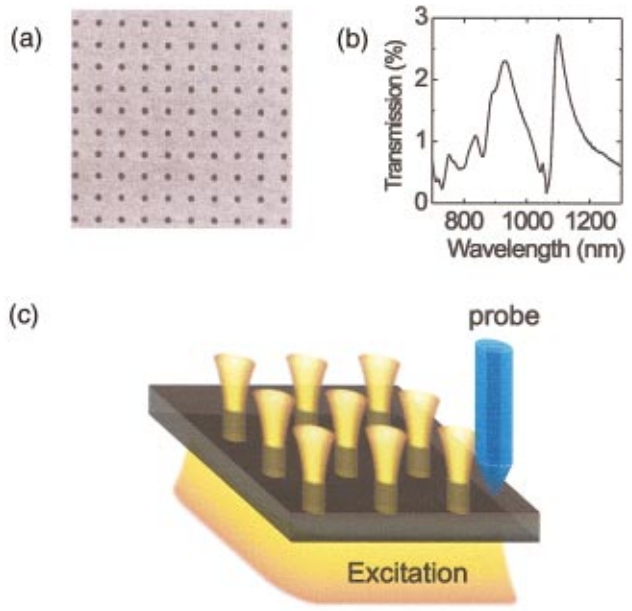

FIG. 1. (Color) (a) Scanning electron microscope image of a typical periodic array of holes in a thick metal film. (b) Far-field transmission spectrum. Holes with 150 nm diameters were made on 300 nm thick gold films with a period of 850 nm. (c) Schematic diagram of the experiment.

pendences are consistent with the fact that the propagation direction of the SP waves is parallel to the exciting light polarization and that SP waves are mostly longitudinal. In all images most of the light transmitted is found on metal surfaces away from the holes, so that over 90% of the integrated light emission originates from the metal surfaces. This behavior is different from previous observations[10] and recent theoretical predictions.[16]

It is important to study which part of the near-field pattern can reach the far field where enhanced transmission is observed. We have varied the distance z between the tip and the surface, at a wavelength that is on the high-energy side of the air–metal [1, 0] resonance (877 nm). As Figs. 3(a)–3(d) show, the pattern is preserved well up to $z \simeq 2.2\ \mu$m, which is well over twice the wavelength. In fact, we can observe vertical stripes up to a distance of 5 μm, when the wavelength of the incident light is close to the lattice constant.

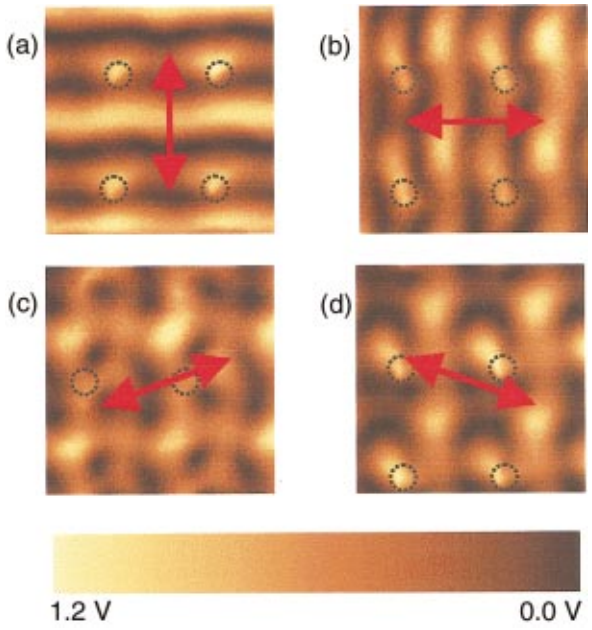

FIG. 2. (Color) Polarization dependence of near-field transmission images near the air-gold [1, 0] and/or [0, 1] resonance using light with wavelength $\lambda = 877$ nm. The data were taken from the same sample as in Fig. 1(b). The arrow represents the polarization of the incident light.

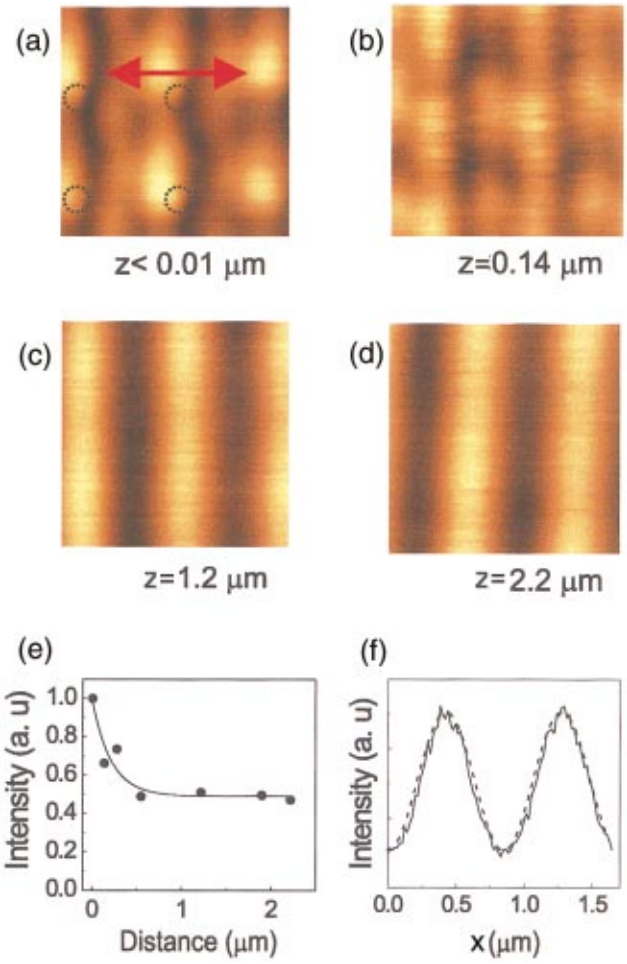

FIG. 3. (Color) Tip–sample distance (z) dependence of transmission images near the air-gold [1, 0] resonance using $\lambda = 877$ nm. The sample is the same as in Fig. 2. (a) $z \lesssim 0.01\ \mu$m. (b) $z \simeq 0.14\ \mu$m. (c) $z \simeq 1.2\ \mu$m. (d) $z \simeq 2.2\ \mu$m. (e) Integrated total transmission as a function of z. (f) Horizontal cross section of (d) (solid line) and the sinusoidal fit (dotted lines).

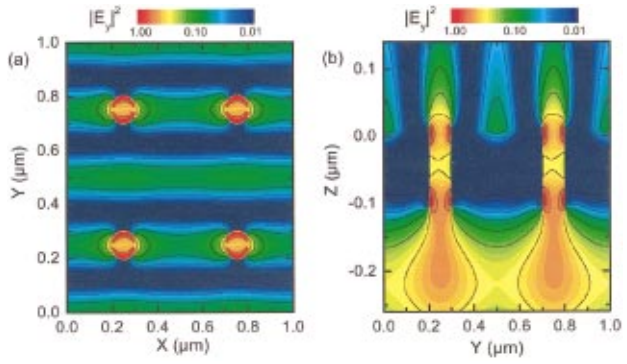

FIG. 4. (Color) Calculated normalized near-field intensity $|E_y|^2$ along one hole array period (on a logarithmic gray scale). (a) $|E_y(x,y,0)|^2$ in the $x-y$ plane showing the SP plasmon field on top of the metal film ($z=0$); (b) cross section $|E_y(x=a_0/2,y,z)|^2$ in the $y-z$ plane on top of the metal film. The cross section is taken along a line ($x=a_0/2$) through the center of the holes.

This clearly indicates that a large portion of the field emanating from nonilluminated metal surfaces is not evanescent: metal shadows can indeed shine into the far field. Figure 3(e) plots the total intensity, spatially integrated over the xy plane, as a function of z. It shows clearly that the light transmitted has both evanescent and nonevanescent components. The evanescent part constitutes about half the total integrated intensity with the decay length of the order of 200 nm.

Figure 3(f) reveals how simple the emission pattern becomes at large z: the cross-sectional intensity of Fig. 3(d) can be fit nearly exactly by $A \pm B \sin(2\pi x/a_0)$ where a_0 is the lattice constant, and A and B fitting parameters. The fact that the region of near-constant integrated intensity of $z \geqslant 0.5\ \mu$m in Fig. 3(e) coincides with the simple patterns of Figs. 3(c) and 3(d) is extremely instructive. In the near field, many in-plane Fourier components, $k_{\|} = 0, \pm 2\pi/a_0$, $\pm 4\pi/a_0$, contribute. That is why the spatial pattern is generally complicated. As z becomes larger, the larger wave vector modes with small penetration depth into the air side all quickly decay out, and only the $k_{\|} = 0, \pm 2\pi/a_0$ modes can survive.

In order to better understand our results, we have performed three-dimensional finite difference time domain (FDTD) simulations of light transmission through 100 nm holes in a free-standing gold film of 100 nm thickness (Fig. 4). The field distributions are calculated for linear y polarization of the incident field by numerically integrating Maxwell equations in the time domain assuming a Drude model for the dielectric function of the metal. For simplicity we chose a lattice constant of the hole array of 500 nm and an excitation wavelength of 530 nm, similar to the experimental conditions. These simulations show [Fig. 4(a)] that the field distribution close to the aperture is described rather well by the Bethe–Boukamp model, and show typical divergence at the rim of the aperture.[1,16] In addition, strong SP fields are generated on the nonilluminated side and the stripe-like patterns run perpendicular to the polarization direction. Interference of the SP field is clearly visible in the local enhancement of the field intensity along lines in the center between adjacent holes, perpendicular to the incident y polarization, as observed experimentally [Fig. 2(a)]. A cross section $|E_y(x=a/2,y,z)|^2$ in the $y-z$ plane along a plane $(x=a/2)$ through the center of the holes is given in Fig. 4(b). The z dependence of the field emitted from the holes and the SP field on the metal surfaces are different. The emission from the holes decays rapidly with an increase in z and it appears that the field that originates from the metal can dominate the far-field emission. The numerical complexity makes it difficult to extend these calculations to the far-field region. Yet, two-dimensional (2D) simulations suggest similar near-field distributions and show indeed a sinusoidally modulated far-field emission that stems from the metal surfaces. The main discrepancy between theory and the experiment is that, in theory, holes are still the brightest spots, whereas in experiments, that is not the case. Clearly more studies are needed.

To summarize, we have shown that nonilluminated metal surfaces away from the periodically arranged holes can shine into the far-field region and preserve its patterns which become essentially sinusoidal. Survival of the first two orders of diffraction and efficient wave vector selection at larger z explain our data. Our experiments are in qualitative agreement with model calculations.

The work in Korea was supported by MOST (the NRL program) and KOSEF (SRC program) and that in Germany by the Deutsch Forschungsgemeinschaft (SFB296) and the European Union through the EFRE and SQID programs.

[1] H. A. Bethe, Phys. Rev. **66**, 163 (1944).
[2] C. J. Bouwkamp, Philips Res. Rep. **5**, 321 (1950).
[3] T. W. Ebbesen, H. J. Lezec, H. F. Ghaemi, T. Thio, and P. A. Wolff, Nature (London) **391**, 667 (1998).
[4] G. Hass, M. H. Francombe and R. W. Hoffman, *Physics of Thin Films* (Academic, New York, 1977), Vol. **9**, p. 145.
[5] V. M. Agranovich, and D. L. Mills, *Surface Polaritons* (North-Holland, Amsterdam, 1982).
[6] H. Raether, *Surface Plasmons on Smooth and Rough Surfaces and on Gratings* (Springer, Berlin, 1988).
[7] J. R. Sambles, Nature (London) **391**, 641 (1998).
[8] H. F. Ghaemi, T. Thio, D. E. Grupp, T. W. Ebbesen, and H. J. Lezec, Phys. Rev. B **58**, 6779 (1998).
[9] T. J. Kim, T. Thio, T. W. Ebbesen, D. E. Grupp, and H. J. Lezec, Opt. Lett. **24**, 256 (1999).
[10] T. Thio, H. F. Ghaemi, H. J. Lezec, P. A. Wolff, and T. W. Ebbesen, J. Opt. Soc. Am. B **16**, 1743 (1999).
[11] D. E. Grupp, H. J. Lezec, T. W. Ebbesen, K. M. Pellerin, and T. Thio, Appl. Phys. Lett. **77**, 1569 (2000).
[12] U. Schröter and D. Heitmann, Phys. Rev. B **58**, 15419 (1998).
[13] U. Schröter and D. Heitmann, Phys. Rev. B **60**, 4992 (1999).
[14] J. A. Porto, F. J. Garcia-Vidal, and J. B. Pendry, Phys. Rev. Lett. **83**, 2845 (1999).
[15] W.-C. Tan, T. W. Preist, and R. J. Sambles, Phys. Rev. B. **62**, 11134 (2000).
[16] L. Salomon, F. Grillot, A. Zayats, and F. de Fornel, Phys. Rev. Lett. **86**, 1110 (2001).
[17] L. Martin-Moreno, F. J. Garcia-Vidal, H. J. Lezec, K. M. Pellerin, T. Thio, J. B. Pendry, and T. W. Ebbesen, Phys. Rev. Lett. **86**, 1114 (2001).
[18] Y. Takakura, Phys. Rev. Lett. **86**, 5601 (2001).
[19] S. J. McNab, R. J. Blaikie, and M. M. Alkaisi, J. Vac. Sci. Technol. B **18**, 2900 (2000).
[20] M. M. Alkaisi, R. J. Blaikie, S. J. McNab, R. Cheung, and D. R. S. Cumming, Appl. Phys. Lett. **75**, 3560 (1999).
[21] W. L. Barnes, T. W. Preist, S. C. Kitson, and J. R. Sambles, Phys. Rev. B **54**, 6227 (1996).
[22] Q. Cao and P. Lalanne, Phys. Rev. Lett. **88**, 05740 (2002).